Global NEST Journal, Vol 26, No 8, 05273

Numerical and experimental analyses for performance and emissions assessment of a four-stroke engine powered by oleic acid methyl ester biofuel made from waste frying oil

Munaf D. F. Al-Aseebee[a,b]*, Ahmed Ketata[b,c], Ahmed Samir Naje[a], Ahmed E. Gomaa[d], Zied Driss[b], Mohamed Salah Abid[b], Haitham Mohamed Emaish[d] and Ahmed M. A. Almaqsub[e]

[a]College of Engineering, AL-Qasim Green University, Babylon 51013, Iraq.

[b]Laboratory of Electromechanical Systems (LASEM), National School of Engineers of Sfax (ENIS), University of Sfax (US), B.P. 1173, Road Soukra km 3.5, 3038 Sfax, Tunisia.

[c]Preparatory Institute for Engineering Studies of Gabes, University of Gabes, Tunisia.

[d]Department of soil and agricultural chemistry, bio system engineering, faculty of agriculture (Saba basha), Alexandria University, P.O. Box 21531, Alexandria, Egypt.

[e]Iraqi Ministry of Education, Wasit Education Directorate.

Received: 31/07/2023, Accepted: 12/08/2024, Available online: 22/08/2024

*to whom all correspondence should be addressed: e-mail: manafal_asseby@wrec.uoqasim.edu.iq, munaf.alaseebee@enis.tn

https://doi.org/10.30955/gnj.05273

Graphical abstract

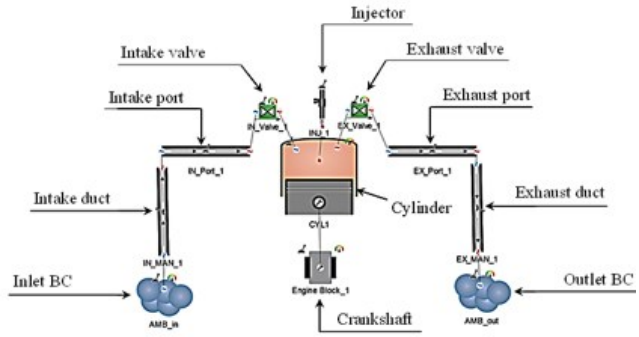

Abstract

Recently, several earlier works conducted research works dedicated to replacing fossil-based fuels with environmentally friendly ones. The goal of the research is to construct a multivariate linear regression model for the attributes of a four-cylinder diesel engine fueled by biodiesel. In this context, the goal of the research is to structure a multiple linear regression example for characterizing a four-cylinder engine fueled by biodiesel. In fact, experimental research was conducted on an agricultural tractor equipped with a 4-cylinder direct-injection diesel engine. The biodiesel is made from waste frying oil without blending referred to as the oleic acid methyl ester (OAME) biofuel. The biodiesel was extracted through a chemical transesterification reaction. The four-stroke engine is tested for both pure OAME biofuel and conventional diesel. One-dimensional numerical simulations were conducted. A strong correlation between numerical and experimental data was observed, validating the numerical model. Using the engine model, in-cylinder pressure, heat release rate, in-cylinder temperature, and emissions including Carbon monoxide (CO), nitrogen oxides (NO_x), and Carbon dioxide (CO_2) were recorded across a broad range of engine operating speeds. Additionally, brake-specific fuel consumption (BSFC) and brake power were numerically calculated and compared to experimental data. The results showed that usage of the OAME as a biofuel could be a promising solution that enables similar performances with lower CO emissions compared to petroleum diesel particularly at low engine speeds.

Keywords: Oleic acid methyl ester, Biodiesel, Transesterification, Diesel, 1-D Numerical model, Four-stroke engine, Performance, Emissions.

1. Introduction

Last years, there is a rising world's need of energy, necessitating increased creative work on cutting-edge renewable energy frameworks for oil-based energy (Hezam, Vedala *et al.* 2023). The world population is increasing and it is anticipated to increase in the future

(Hajjari, Tabatabaei *et al.* 2017). This growing population is due to the world's energy demands as well. According to the Energy Information Administration (EIA), around 87% of global energy consumption is met by fossil fuels, including coal, natural gas, and petroleum oils (Sourmehi 2021). These petroleum gasoline stocks are continuously depleting as they are not regenerative (Raju, Veza *et al.* 2023). In addition, using fossil fuels excessively resulted in significant global climate change [Jia, Cheng *et al.* (2023), (Rattanaphra, Tawkaew *et al.* 2023)]. An intense pressing energy need arises to identify sustainable energy sources to meet this increasing energy demand [(Musharavati, Sajid *et al.* 2023), (Zailani, Iranmanesh *et al.* 2019)]. So, it is necessary to have research on the replacement of fossil fuels with biofuels that have lesser impacts on the environment [(Dey, Singh *et al.* 2023), (Etim, Betiku *et al.* 2018)]. In 2020, the United States of America (USA) became the leading biodiesel producer, producing 200,000 barrels daily, 48% of the world's total biodiesel production (Doppalapudi, Azad and Khan 2024). Followed by Brazil, accounting for 28%, and both Germany and China, accounting for 3 % of the entire world's biodiesel production, respectively (Vickram, Manikandan *et al.* 2023). Indonesia, the largest biodiesel producer in 2022, mainly used palm oil as the feedstock for biodiesel production (Doppalapudi, Azad and Khan 2024). According to the International Energy Agency (IEA) forecasts, the current production rate, the need for biodiesel will increase by 52.9 billion liters in the next five years (Doppalapudi, Azad and Khan 2024). As for the expedited example, the demand will increase by 68.1 billion liters by 2028 (Doppalapudi, Azad and Khan 2024). Extensive research studies have been conducted worldwide for the non-edible feedstock is termed as the second-generation feedstock for biodiesel production (Azad, Jadeja *et al.* 2024). Among all different biofuels, biodiesel has sparked much interest and fame among the various alternative fuel options [(Ahmad, Imran *et al.* 2023), (Azad, Halder *et al.* 2023)]. Therefore, maximizing the development and utilization of biodiesel may be a potential solution to the current problem [(Doppalapudi, Azad and Khan 2021) - (Rahman, Kamil and Bakar 2011)]. The physicochemical properties of the biodiesel vary with the feedstock type, and plenty of another feedstock. Selected Tucuma and Ungurahui as new feedstocks because of their high lipid fat content. Their application in diesel engines was tested and presented in the following studies [(Dhar and Agarwal 2015) – (Singh, Sharma *et al.* 2019)]. Biodiesel fuels have demonstrated several interesting factors due to their physical composition, operating conditions, and their blend ratios for mixing the blend. For instance, Habibullah, Masjuki *et al.* (2014) conducted experimental analysis with coconut and palm oil biodiesels blended with diesel. This study reported a reduction in CO and HC by 13.75 % and 17.97 %, respectively, for both fuels compared to diesel fuel. However, according to the study of Habibullah, Masjuki *et al.* (2014), palm oil has higher NOx than coconut biodiesel. All these biodiesels produced from several renewable sources meet the standard specifications imposed by the American Society for Testing and Materials ASTM D6751 standard (McCormick, Alleman and Nelson 2023). Biodiesels are non-toxic and biodegradable [(Doppalapudi, Azad and Khan 2024), (Doppalapudi, Azad and Khan 2023)]. For example, various feedstock's such as babassu, andiroba, almond, tamanu, camelina, copra, coconut fish oil, jatropha, groundnut, microalgae, Karanja, oat, sesame, poppy seed, and sorghum are used in many studies to produce biodiesel esters [(Abu-Hamdeh and Alnefaie 2015)–(Patel and Sankhavara 2017)]. Many methods are used to change biodiesel, including thermochemical, biochemical, and electrochemical conversion [(Azad 2017), (Ghadge and Raheman 2006)]. The most effective method is the transesterification method, which follows the thermochemical conversion process, where triglyceride molecules react with alcohol in the presence of a catalyst. This chemical conversion process converts fatty acids to esters and glycerin (Abbaszaadeh, Ghobadian *et al.* 2012). Base catalysts such as sodium hydroxide and potassium hydroxide were widely used in commercial applications (Ghedini, Taghavi *et al.* 2021). Many studies have focused on modeling the biodiesel production process, and several more have argued energy consumption, mass and heat integration methods, economic evaluation, and life cycle assessment [(Lee, Posarac and Ellis 2011), (Apostolakou, Kookos *et al.* 2009) - (Vlysidis, Binns *et al.* 2011)]. However, there are very few studies on the production plant design and the fluid flow losses that relate to the conversion process.

The present study aimed to manufacture biodiesel fuel and testing under different engine conditions. The biofuel was tested in a 67 kW four-cylinder Kubota diesel tractor engine at the Agricultural Engineering Research Institute (AERI) in Alexandria, Egypt. Moreover, the present investigation relies on a simple computational 1-D approach validated to test data to achieve the main goal of this study. Based on the obtained results, the variation in the instantaneous engine in-cylinder characteristics, performance and emissions such as the brake power, and NOx, CO, CO2 emissions have been analyzed under a wide range of engine speed. According to the results, the biodiesel production process is acknowledgeable, and help to reduce the overall production cost. In addition, the manufactured biofuel contributed to a significant reduction in the engine emissions while conserving comparable performance to conventional diesel.

2. Experimental study

In this study, the biodiesel, consisting of the oleic acid methyl ester (OAME), was manufactured from waste frying oil through the transesterification reaction as illustrated in Figure 1a.

The transesterification process involves converting an organic ester group into an organic alcohol group. The addition of an acid or base catalyst often catalyzes this reaction. After the produced reaction, glycerol and methyl esters can be separated using a centrifuge or a settling tank. Figure 1b shows the state of the mixture after the end of the separation step between the glycerol and the ester due to the low solubility of the ester, making it simple and rapid to separate. The residual methanol that did not react

serves as a solvent. Figure 1c depicts a view of the final state of the OAME biodiesel product after a process of washing with distilled water and separation based on heating. A KUBOTA agricultural tractor equipped with a conventional four-cylinder diesel engine was used for testing the produced OAME Biodiesel and its effects on the overall performance and emissions of internal combustion engines (ICE). Table 1 shows the technical specifications of the KUBOTA tested engine. Figure 2a depicts an actual view of the KUBOTA agricultural tractor engine under test fed with the OAME biofuel. A hydraulic brake dynamometer, as shown in Figure 2b, was used to measure brake torque. The engine was experimentally tested using 100% fuel made from used cooking oil and the results were compared with conventional diesel fuel, as reported in the research (Al-Aseebee, Ketata *et al.* 2023).

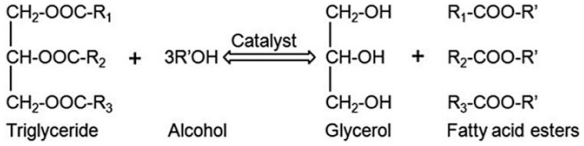

(a) Transesterification reaction

(b) Separation between glycerol and methyl ester

(c) Final OAME biodiesel product

Figure 1. OAME biodiesel production.

(a) Engine of KUBOTA agricultural tractor fed with OAME biofuel

(b) Hydraulic dynamometer

Figure 2. Experimental study of OAME biofuel on the KUBOTA agricultural tractor.

Table 1. Technical specifications of the Kubota engine.

Type of engine	Four strokes, liquid-cooled diesel
Compression ratio	21.8:1
Number of cylinders	4-cylinder
Bore (mm)	100
Stroke (mm)	120

3. Performance parameters

3.1. Brake torque and power

The engine brake power P_b was calculated from the generated electrical power P_e in the dynamometer considering its mechanical efficiency n_m as follows:

$$P_b = \frac{P_e}{n_m} \quad (1)$$

The brake power P_b is related to the brake torque τ_b by the following formula:

$$P_b = \frac{2\pi N}{60}\tau_b \quad (2)$$

3.2. Brake specific fuel consumption

Figure 5a shows the variation in brake-specific fuel consumption (BSFC) of the tested engine concerning the engine speed for different diesel and biodiesel blends examined. The BSFC, expressed in g.kWh^{-1} as a unit, was calculated as follows:

$$BSFC = 3.610^6 \frac{r}{P_b} \quad (3)$$

Where r is the fuel consumption in grams per second and P_b is the brake power in Watt.

3.3. Heat release rate (HRR)

Heat Release Rate (HRR) is a critical factor in analyzing the combustion phenomenon inside the engine cylinder. HRR reflects the chemical energy of the fuel that is converted into thermal energy. The Heat Release Rate (HRR) in the engine cylinder relies on factors such as the peak pressure rise, premixed rapid combustion, and ignition delay. Generally, a longer ignition delay leads to a greater accumulation of experimental fuel during the pre-mixed combustion phase, resulting in increased pressure and temperature during the subsequent uncontrolled rapid combustion. (Nathan, Mallikarjuna and Ramesh 2010). The HRR per crankshaft (CA) angle denoted as $\frac{dQ}{d\theta}$, is modeled by applying the first law of thermodynamics and can be given as follows (Sanjid, Kalam *et al.* 2014, Kale 2017):

$$\frac{dQ}{d\theta} = \frac{\gamma}{\gamma - 1} P \frac{dV}{d\theta} + \frac{1}{\gamma - 1} V \frac{dP}{d\theta} \quad (4)$$

Where Q is the released heat, θ is the crankshaft angle, P is the in-cylinder pressure, V is the cylinder volume, γ is the specific heat ratio of the fuel-air mixture.

4. Computational method

In this work, the engine under test has been modeled using a one-dimensional (1-D) gas dynamics engine model of the Ricardo Wave environment, which uses a staggered grid finite-volume discretization method. Various programs, from model setup to output analysis, are needed to use the 1-D engine package. Three programs were used in this study: Wave Post was used to post-process the results, Wave Build GUI was used to model the engine, and Wave Solver was used to solve the flow governing equations. Figure 3 shows a view of the 1-D engine model built with the Ricardo Wave Build GUI. The present engine model is made up of several sub-models of the intake and exhaust ducts, the intake and exhaust valves, the injector, the single cylinder, and the crankshaft, as illustrated in Figure 3.

This model is most likely like the 1-D diesel engine model that was previously constructed by (Ketata, Moussa and Driss 2023). The thermodynamic parameters of each fuel are put down in a ".data" file, which is created for both

conventional diesel and biofuel. The flow conservation equations, which are composed of the momentum, enthalpy, and continuity equations, were solved with the goal of getting the flow solution in the input and exhaust ducts.

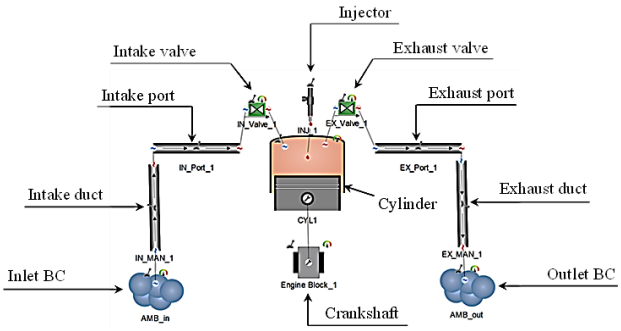

Figure 3. Schematic layout of the 1-D engine model.

$$\frac{\partial m}{\partial t} = \sum_{\text{boundaries}} \dot{m} \tag{5}$$

$$-Adp + \sum_{\text{boundaries}} (\dot{m}u) \tag{6}$$

$$\frac{\partial \dot{m}}{\partial t} = \frac{-4C_f \dfrac{\rho u|u| dx A}{2D} - \dfrac{1}{2} k_p \rho u|u| A}{dx}$$

$$\frac{\partial (\rho H u)}{\partial t} = \sum_{\text{boundaries}} \dot{m}H + u\frac{dp}{dt} - hA(T_f - T_w) \tag{7}$$

Where m the fluid is mass, $\dot{m}$ is the mass flow rate, u is velocity, ρ is density, H is the total enthalpy and t is time. T_f Is the fluid static temperature, p is static pressure, C_f is the Fanning friction coefficient, T_w is the wall temperature, k_p is the pressure loss coefficient and h is the heat transfer coefficient. D Is the equivalent hydraulic diameter and A is the pipe section of any cross-sectional shape.

In simulations, the maximum admissible time step size is found for each sub-volume of the computing domain using the Courant condition CFL. The following is the condition that is applied to the time stepdt:

$$dt = CFL\frac{dx}{(c + mod(v))} \tag{8}$$

Where dx is the discretization length, c is the speed of sound and v is the instantaneous gas velocity.

The engine cylinder's heat transport was modeled using the well-known Woschni's model. The heat transfer coefficient, h_c, can be computed using this model in the following way:

$$h_c = \frac{K_1 p^{0.8} u^{0.8}}{B^{0.2} T^{K_2}} \tag{9}$$

Where k_1 and k_2 are constants of the model equal to 3.014 and 0.5 respectively, p is the in-cylinder pressure, B is the cylinder bore, T is the in-cylinder temperature, and u is the average cylinder gas velocity.

Based on the three-term Wiebe function obtained from the superposition of the three normal Wiebe curves, the burn rate for direct-injection compression-ignition engines was computed. These Wiebe curves roughly stands for the principal single injection burn rate and the form of a Direct Injection (DI) compression ignition. Three functions are used to enable modeling the premixed and diffusion phases of the combustion process. The cumulative burn rate was computed using this model in the following way:

$$BR(\theta) = \eta_c \begin{pmatrix} F_p\left[1 - e^{-W_{cp}(\theta - S_{oi} - I_d)^{E_p+1}}\right] \\ + F_m\left[1 - e^{-W_{cm}(\theta - S_{oi} - I_d)^{E_m+1}}\right] \\ + F_t\left[1 - e^{-W_{ct}(\theta - S_{oi} - I_d)^{E_t+1}}\right] \end{pmatrix} \tag{10}$$

Where η_c is the combustion efficiency, θ is the crankshaft angle, I_d is the ignition delay, S_{oi} is the start of the ignition angle. E_p, E_m and E_t are the Wiebe premix, main and tail exponents respectively. W_{cp}, W_{cm}, and W_{ct} are the Wiebe premix, main and tail constants respectively. F_p, F_m, and F_t are the Wiebe premix, main and tail fractions respectively.

The main Wiebe fraction F_m calculated is as follows:

$$F_m = 1 - F_p - F_t \tag{11}$$

The Wiebe premix, main, and tail constants were calculated as follows:

$$W_{cp} = \left(\frac{D_p}{2.302^{1/E_p+1} - 0.105^{1/E_p+1}}\right)^{-(E_p+1)} \tag{12}$$

$$W_{cm} = \left(\frac{D_m}{2.302^{1/E_m+1} - 0.105^{1/E_m+1}}\right)^{-(E_m+1)} \tag{13}$$

$$W_{ct} = \left(\frac{D_t}{2.302^{1/E_t+1} - 0.105^{1/E_t+1}}\right)^{-(E_t+1)} \tag{14}$$

Where D_p, D_m, and D_t are the Wiebe premix, main and tail durations respectively.

A huge output file including all the information needed to examine the simulated engine action is generated once a simulation has reached convergence. The outcomes are then plotted using the Ricardo Wave Post.

5. Results and discussion

5.1. Numerical validation

Figure 4 shows a comparison between the numerical and experimental values of the brake power for both conventional diesel and produced OAME biodiesel. The purpose of this analysis is to find the necessary relevant information to use in justifying the numerical results. From these results, it has been observed a good match between the numerical and experimental results. For both conventional diesel and produced OAME biodiesel, the deviation of the numerical results to test data did not exceed 10%, which ensures the validity of the computational approach. The conventional diesel showed a better output brake power compared to the OAME biodiesel. The brake power recorded for the conventional diesel stills a little bit higher than that recorded for the OAME biofuel. This observation is more prominent at medium rotational speed range of the engine from 1500 rpm up to 2500 rpm. However, the difference in the brake power seems to be negligible at low and high rotational speed of the engine. Overall, the brake power obtained

from the produced OAME biodiesel can be considered competitive to that for the diesel fuel.

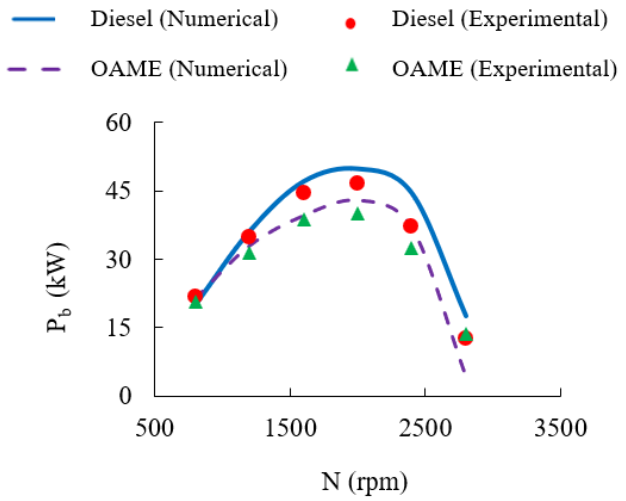

Figure 4. Comparison of cycle-average brake power to test data for both conventional diesel and OAME biofuel.

5.2. Instantaneous characteristics

5.2.1. In-cylinder pressure

Cylinder pressure is a good indicator of the ability to mix air with fuel. Figure 5 shows the instantaneous change in the pressure inside the cylinder as a function of the crankshaft angle (CA) for both the conventional diesel fuel and the produced OAME biodiesel for the six investigated engine rotational speeds from 800 rpm up to 2800 rpm. Based on these results, it is worth noting that both fuels show practically similar trend of the in-cylinder pressure except for the zone 25° and 100° after the top dead center (TDC). This zone can be referred to the difference of the physicochemical properties between the pure petroleum diesel and the produced OAME biodiesel. Nevertheless, the peak value of the in-cylinder pressure occurring near the TDC is found to be similar for both fuel cases. For instance, under a rotational speed of 2400 rpm as shown in Figure 5e, the maximum pressure for the OAME biodiesel is of 109.3462 bars concurring at 0.3194 deg before the top dead center. While the maximum pressure for the conventional diesel fuel recorded a similar result of 109.3404 bar at 0.3165 deg before the top dead center. These results are consistent with the studies previously conducted by Fournier, Simon and Seers (2016) and López, Cadrazco *et al.* (2015).

5.2.2. Cumulative heat release

Figure 6 shows the variation of the cumulative heat release with respect to the crankshaft angle (CA) for both the conventional diesel fuel and the produced OAME biodiesel under an engine rotational speed range from 800 rpm up to 2800 rpm. The released heat shows the ability of the fuel chemical energy to be converted into thermal energy. From these results, it was shown a lower released heat from the produced OAME biodiesel in comparison to the conventional diesel fuel during combustion, particularly at low and high rotational speeds. This difference in heat generation becomes less significant at medium speed range. As an example, under an engine speed of 2400 rpm, it has been observed that the maximum cumulative heat release for the produced OAME biodiesel is 2.53 kJ. Meanwhile the maximum cumulative heat release for the conventional diesel fuel recorded a decreased value of 1.76 kJ as illustrated in Figure 6a. The viscosity is considered the key factor for this behavior because it produces slower combustion, reducing heat release. Similar behavior was obtained in the investigation of Can (2014).

5.2.3. In-cylinder temperature

The in-cylinder temperature is an important thermodynamic parameter that significantly affects the mechanical and thermal stresses of the different parts of the engine as well as its emissions as also confirmed by the study of Srivastava, Kesharvani *et al.* (2023). Figure 7 depicts the instantaneous change in the in-cylinder temperature with respect to the crankshaft angle (CA) for both the conventional diesel fuel and the produced OAME biodiesel under an engine rotational speed range from 2800 rpm down to idle at 800 rpm. The in-cylinder temperature gradually increases during the compression stroke from bottom dead center (BDC) up to 7° before the TDC. As the injectors spray the fuel into the cylinder, the in-cylinder temperature slightly decreases. Once the combustion reaction is started, the temperature increases with a steep slope until it reaches its peak value at about 40° after the TDC. Then, the temperature starts to decrease with a stepper slope during the expansion stroke. In addition, it has been reported that the produced OAME biodiesel leads to lower combustion temperature compared to the pure diesel for all investigated rotational speeds of the engine.

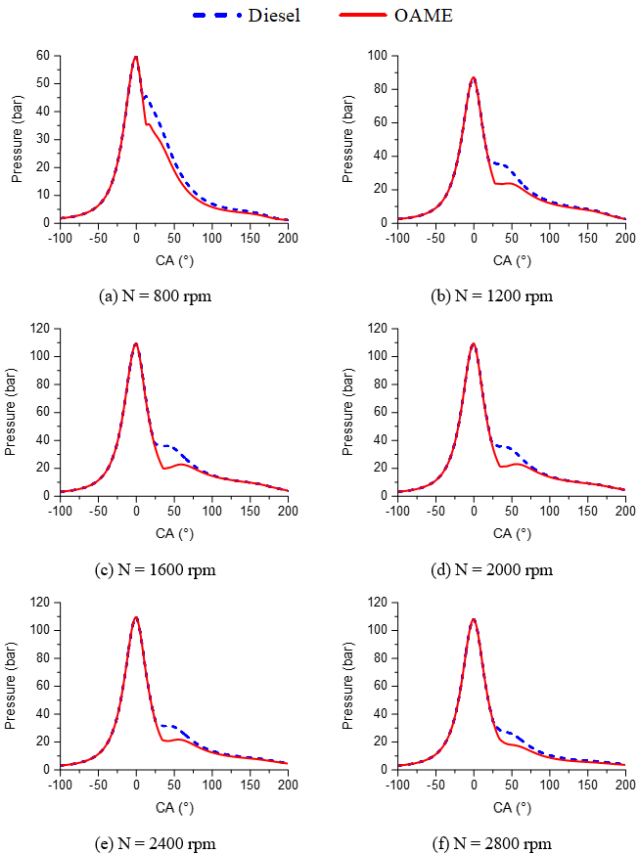

Figure 5. Instantaneous in-cylinder pressure versus the crankshaft angle (CA) for six different engine rotational speeds.

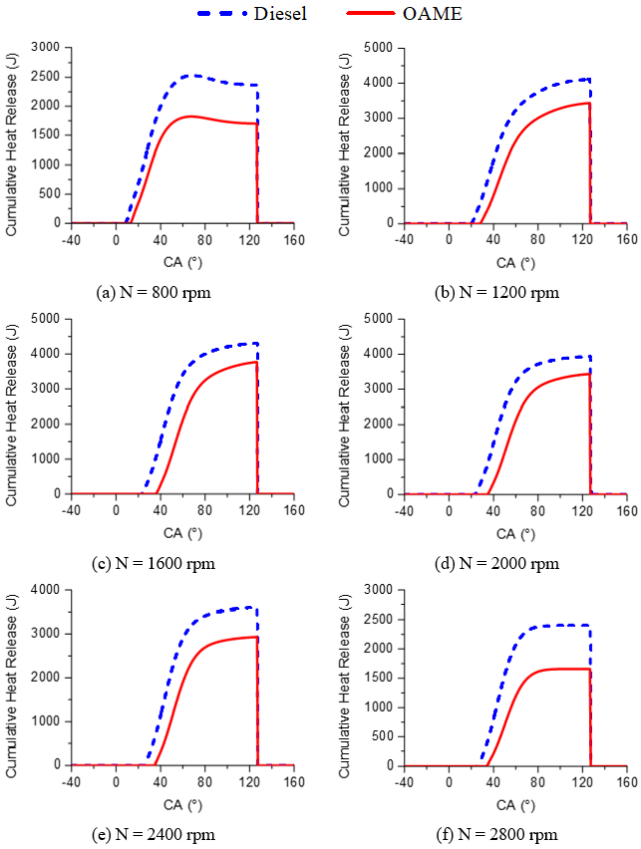

Figure 6. Instantaneous cumulative heat release versus the crankshaft angle (CA) for six different engine rotational speeds.

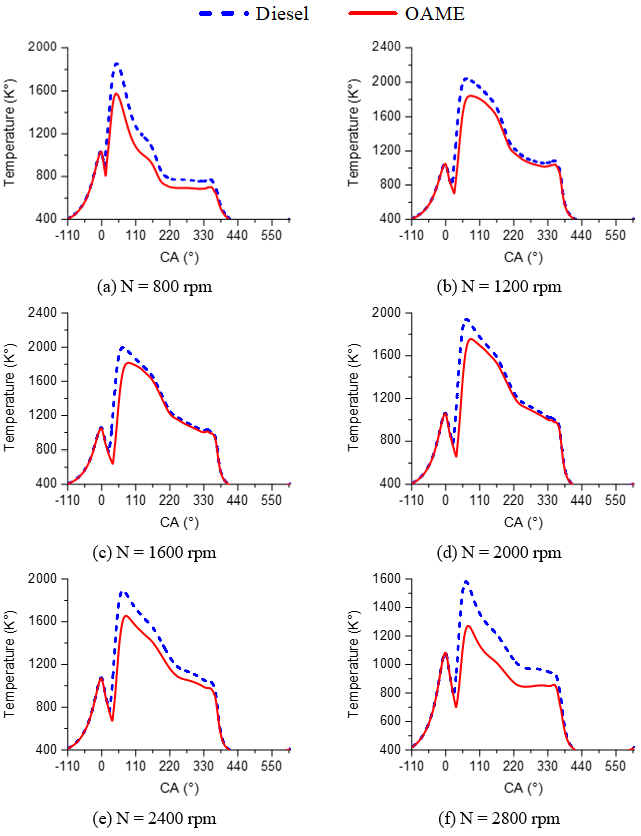

Figure 7. Instantaneous in-cylinder temperature versus the crankshaft angle (CA) for six different engine rotational speeds.

As an instance, un an engine rotational speed of 800 rpm, it was registered a value of the maximum in-cylinder temperature for the produced OAME biofuel of 1580 K, while the maximum in-cylinder temperature for the conventional diesel fuel is of 1855 K. These results are attributed to the lower calorific value of the produced OAME biofuel compared to petroleum diesel. These results are in a good accordance with those previously reported by Zhang, Yan *et al.* (2022).

5.3. Cycle-average performance

5.3.1. Brake power

The properties of biodiesel, particularly its heating value and viscosity, directly influence engine brake power components. The heating value of a fuel is a crucial indicator of the energy available for generating work. Consequently, biodiesel has a lower heating value resulting in a reduced engine power output. Figure 8 shows the variation of brake power (BP) with respect to the engine rotational speed for both the conventional diesel fuel and the produced OAME biodiesel.

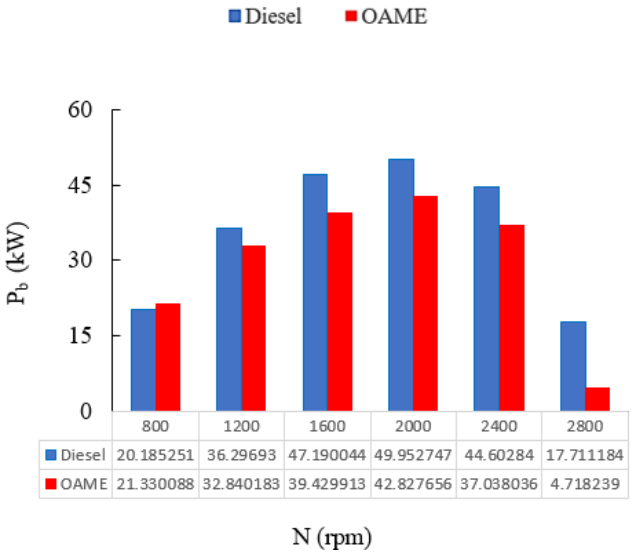

Figure 8. Cycle-average Brake power.

It can be seen from the graph illustrated in Figure 8 that the brake power increases with an increasing engine speed until it reaches its maximum value at the speed of 2000 rpm and then decreases to reach its lowest value at the speed of 2800 rpm. It was noted that the maximum brake power for conventional diesel fuel is 49.952 kW under an engine rotational speed of 2000 rpm, while the maximum brake power for the OAME biofuel was recorded as 42.728 kW at the same speed. The lowest value of 17.711 kW was for conventional diesel fuel. However, the lowest value for the OAME biofuel of 4.718 W. Overall, the results show that the adoption of the OAME biodiesel as a replacement of the petroleum diesel leads to a slight reduction in the output power of the engine. These results are consistent with what was previously mentioned by Gomaa, Mohamed *et al.* (2014), Ketata, Moussa and Driss (2023).

5.3.2. Brake specific fuel consumption

Figure 9 shows the distribution of the brake-specific fuel consumption (BSFC) for both the conventional diesel fuel and the produced OAME biodiesel at different speeds ranging from 800 to 2400 rpm. The maximum BSFC value for the OAME biodiesel is of 757.833 GkWh^{-1} at 2400 rpm. The maximum BSFC value for fossil diesel is 549.061

g.k.W.h^{-1} at 800 rpm. The lowest value for fossil diesel at 1600 engine rpm is 409.374 GkWh^{-1}, while the lowest value for the OAME biodiesel is 530.006 GkWh^{-1} at 1200 engine rpm.

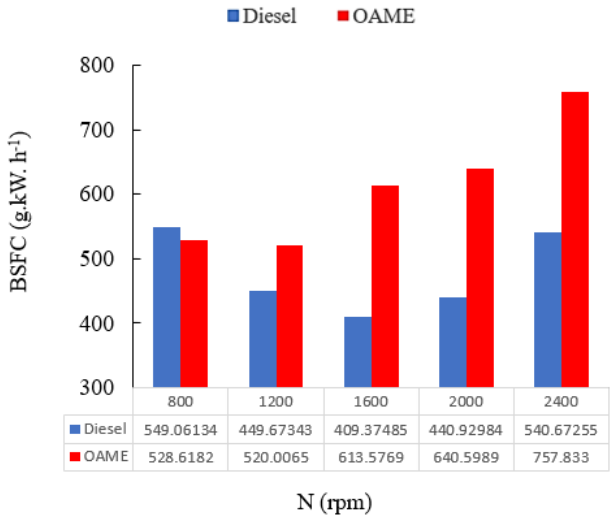

Figure 9. Cycle-average value of the brake-specific fuel consumption (BSFC).

Based on these results, it can be stated that the usage of the OAME biofuel as a replacement of petroleum diesel led to an increase in engine consumption. This fact is due to the lower heating value per unit mass of the biodiesel compared to diesel fuel. These results are in a good accordance with the finding of (McCarthy, Rasul and Moazzem 2011).

5.4. Cycle-average emissions

5.4.1. Carbon oxide

Figure 10 shows the cycle-average value of the emissions of carbon monoxide (CO) given in percentage for both the conventional diesel and the produced OAME biodiesel at different engine speeds.

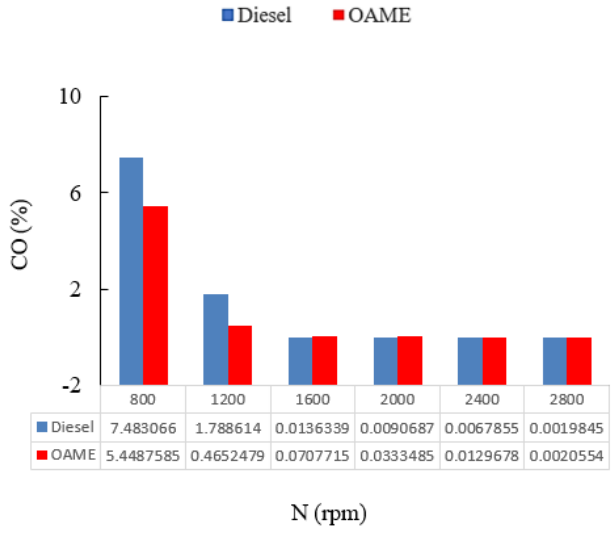

Figure 10. Cycle-average value of CO emission.

It has been noted that the engine rotational speed affects the CO emission because the temperature of the gas cylinder decreases when engine speed decreases, causing the conversion of carbon monoxide oxidation to carbon dioxide to slow down. Therefore, an increase in CO emission at low speeds was noticed. Increasing the engine rotational speed leads to a significant rise in the fuel consumption and the in-cylinder temperature. The conventional diesel fuel recorded the maximum carbon monoxide emissions, reaching 7.483% compared to the produced OAME biodiesel, where the CO emission reached 5.448% at the engine speed of 800 rpm. The lowest CO emission was for the conventional diesel fuel, which reached 0.0019%, while the lowest percentage for the OAME fuel was about 0.0020%, both at the engine speed of 2800 rpm. As a deduction, it can be reported that the usage of the produced OAME biofuel has led to a significant decrease in the CO emission compared the petroleum diesel. These results match well the previous research work of Gad, El-Shafay and Hashish (2021).

5.4.2. Carbon dioxide

Figure 11 shows the cycle-average value of the emissions of carbon dioxide (CO_2) given in percentage for both the conventional diesel and the produced OAME biodiesel for the six investigated engine speeds. The graph shows that the emission percentage of CO_2 of the conventional diesel is like that of the produced OAME biofuel. The percentage of CO_2 greatly increases at high temperatures during combustion, as carbon bonds are broken and new bonds are formed with oxygen atoms and release more chemical energy and water (A Zayed, SM Abd El-Kareem and Zaky 2016). Under an engine speed of 1200 rpm, the OAME fuel recorded the highest value for the CO_2 emission, reaching 9.305%, compared to the conventional diesel fuel, which recorded the highest value about 8.364%. The lowest recorded value of the CO_2 emission was for the OAME biofuel, which amounted to 4.365%, while for the conventional diesel fuel, the lowest recorded value was 5.108%, both at the engine speed of 2800 rpm.

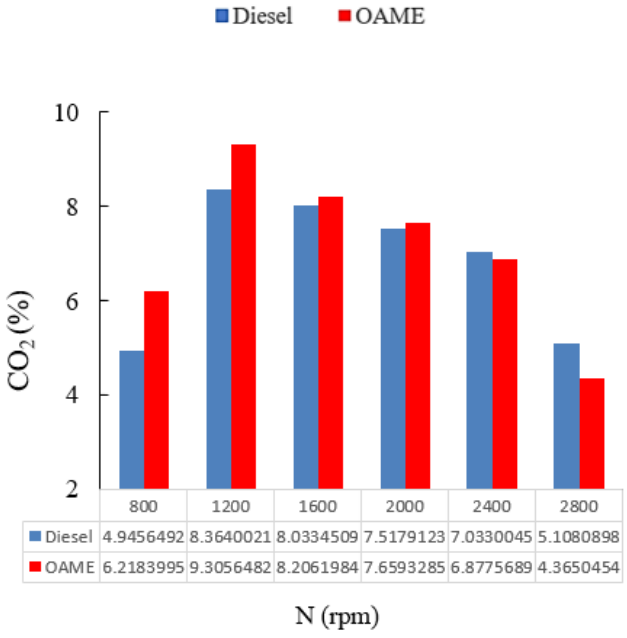

Figure 11. Cycle-average value of the CO_2 emission.

5.4.3. Nitrogen oxide

Figure 12 shows the cycle-average value of the emissions of nitrogen oxide (NO_x) given in ppm for both the conventional diesel and the produced OAME biodiesel for

the six investigated engine speeds. The produced OAME biofuel recorded the highest NOx emission value, reaching approximately 1899.4 ppm, compared to the conventional diesel fuel, which recorded the value of 1088.86 ppm under an engine speed of 1600 rpm. The lowest recorded NOx emission value was found for the OAME biofuel, amounting to 44.28 ppm, while for the conventional diesel fuel, the lowest recorded value was about 28 ppm, both at the idle rotational speed of about 800 rpm. Hence, it can be reported that the increase in NOx emission is related to the increase in the in-cylinder temperature. Indeed, the NO_x formation significantly depends on the cylinder temperature since the medium speeds recorded the maximum temperature values of combustion. At low engine speeds, the fuel-air mixture is lean with a greater concentration of oxygen, but the fuel-air mixture is rich at high engine speeds.

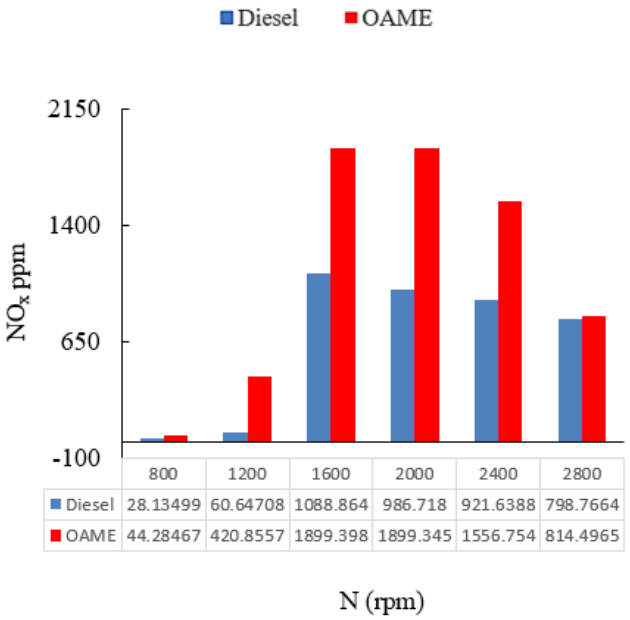

	800	1200	1600	2000	2400	2800
Diesel	28.13499	60.64708	1088.864	986.718	921.6388	798.7664
OAME	44.28467	420.8557	1899.398	1899.345	1556.754	814.4965

Figure 12. Cycle-average value of the NO_x emission.

The separated nitrogen reacts with oxygen at the higher cylinder combustion temperature and leads to the formation of thermal NOx. At higher engine speeds, the reaction time is reduced so that the residence time is shortened resulting in lower NOx emission. The decrease in the NOx emission with an increasing engine speed was due to the lower oxygen content and lower reaction time. In addition, it can be noted that the higher cetane number and shorter ignition delay of the produced OAME biofuel compared to the conventional diesel fuel resulted in increased NOx emissions.

6. Conclusion

In this work, the impact of a produced OAME biodiesel on the performance and emissions of internal combustion engines was investigated under a wide range of the rotational speed. The OAME biodiesel was produced with the transesterification reaction, and it was compared to the petroleum diesel through both experimental and numerical studies. The experimental study was carried out with a KUBOTA agricultural tractor equipped with a conventional four-cylinder diesel engine. A 1-D engine numerical model is developed to study the effect of the produced OAME biodiesel on the engine instantaneous characteristics. The standard deviation (SD) of the numerical results ranges from 0% up to 10%. As the deviation does not reach a value above 10%, the numerical simulation can be considered valid for predicting the engine performance under different fuels with an acceptable accuracy. Based on the numerical and experimental results, it has been drawn the following outcomes:

Similar instantaneous in-cylinder pressure profiles were recorded with small discrepancies confirming that the biodiesel has not any significant effect on the pressure distribution inside the cylinder.

The comparison of the instantaneous in-cylinder temperature and the cumulative heat release revealed a decreasing heat release up to 30% as the produced OAME is being used to feed the engine. This fact was explained by the lower calorific value of the biodiesel compared the petroleum diesel.

A reduction up to 14% of the engine brake power at high and mid-range engine rotational speeds was recorded as the engine is fed with the produced OAME biodiesel compared to the traditional diesel fuel.

The use of the produced OAME biofuel has led to an increasing fuel consumption by an amount of 50% particularly at high and medium engine speeds. At low engine speeds, the fuel consumption is similar to that found for the petroleum diesel.

The emissions of both carbon monoxide (CO) are significantly mitigated at low engines speeds with the usage of the produced OAME biodiesel. The lost quantity of CO emissions was converted into carbon dioxides (CO_2) by means of the oxidation reaction. Thus, the emission of carbon dioxide (CO_2) registered slightly higher value for the OAME biofuel compared to the traditional fossil diesel.

A significant increase, up to 90%, in the nitrogen oxide (NO_x) emission was noted when the produced OAME biofuel was used. This observation is due to the high content of oxygen in the produced biodiesel.

This current research work suggests that biodiesel can be an environmentally friendly fuel that does not necessarily have to completely replace petroleum diesel but can be partially added to the diesel fuel in a certain proportion to keep low carbon oxide (CO) emissions while keeping approximately the same performance.

References

Abbaszaadeh A., Ghobadian B., Omidkhah M. R. and Najafi G. (2012). "Current biodiesel production technologies: A comparative review." *Energy Conversion and Management* **63**: 138–148.

Abu-Hamdeh N. H. and Alnefaie K. A. (2015). "A comparative study of almond biodiesel-diesel blends for diesel engine in terms of performance and emissions." *BioMed Research International* **2015**(1): 529808.

Ahmad G., Imran S., Farooq M., Shah A. N., Anwar Z., Rehman A. U. and Imran M. (2023). "Biodiesel production from waste

cooking oil using extracted catalyst from plantain banana stem via RSM and ANN optimization for sustainable development." *Sustainability* **15**(18): 13599.

Al-Aseebee M. D., Ketata A., Gomaa A. E., Moussa O., Driss Z., Abid M. S., Naje A. S. and Emaish H. H. (2023). "Modeling of waste vegetable oil biodiesel for tractor engine utilization." *Journal of Ecological Engineering* **24**(12).

Apostolakou A., Kookos I., Marazioti C. and Angelopoulos K. (2009). "Techno-economic analysis of a biodiesel production process from vegetable oils." *Fuel Processing Technology* **90**(7–8): 1023–1031.

Azad A. (2017). "Biodiesel from mandarin seed oil: A surprising source of alternative fuel." *Energies* **10**(11): 1689.

Azad A. K., Jadeja A. C., Doppalapudi A. T., Hassan N. M. S., Nabi M. N. and Rauniyar R. (2024). "Design and simulation of the biodiesel process plant for sustainable fuel production." *Sustainability* **16**(8): 3291.

Azad A., Halder P., Wu Q., Rasul M., Hassan N. and Karthickeyan V. (2023). "Experimental investigation of ternary biodiesel blends combustion in a diesel engine to reduce emissions." *Energy Conversion and Management: X* **20**: 100499.

Can Ö. (2014). "Combustion characteristics, performance and exhaust emissions of a diesel engine fueled with a waste cooking oil biodiesel mixture." *Energy Conversion and Management* **87**: 676–686.

Dey S., Singh A. P., Gajghate S. S., Pal S., Saha B. B., Deb M. and Das P. K. (2023). "Optimization of CI engine performance and emissions using alcohol–biodiesel blends: a regression analysis approach." *Sustainability* **15**(20): 14667.

Dhar A. and Agarwal A. K. (2015). "Experimental investigations of the effect of pilot injection on performance, emissions and combustion characteristics of Karanja biodiesel fuelled CRDI engine." *Energy Conversion and Management* **93**: 357–366.

Doppalapudi A. T., Azad A. and Khan M. (2021). "Combustion chamber modifications to improve diesel engine performance and reduce emissions: A review." *Renewable and Sustainable Energy Reviews* **152**: 111683.

Doppalapudi A. T., Azad A. K. and Khan M. (2024). "Experimental investigation on diesel engine performance, combustion, and emissions characteristics with Tucuma and Ungurahui biodiesel blends." *Fuel* **371**: 132161.

Doppalapudi A., Azad A. and Khan M. (2023). "Advanced strategies to reduce harmful nitrogen-oxide emissions from biodiesel fueled engine." *Renewable and Sustainable Energy Reviews* **174**: 113123.

Etim A. O., Betiku E., Ajala S. O., Olaniyi P. J. and Ojumu T. V. (2018). "Potential of ripe plantain fruit peels as an ecofriendly catalyst for biodiesel synthesis: optimization by artificial neural network integrated with genetic algorithm." *Sustainability* **10**(3): 707.

Fournier S., Simon G. and Seers P. (2016). "Evaluation of low concentrations of ethanol, butanol, BE, and ABE blended with gasoline in a direct-injection, spark-ignition engine." *Fuel* **181**: 396–407.

Gad M., El-Shafay A. and Hashish H. A. (2021). "Assessment of diesel engine performance, emissions and combustion characteristics burning biodiesel blends from jatropha seeds." *Process Safety and Environmental Protection* **147**: 518–526.

Ghadge S. V. and Raheman H. (2006). "Process optimization for biodiesel production from mahua (Madhuca indica) oil using response surface methodology." *Bioresource Technology* **97**(3): 379–384.

Ghedini E., Taghavi S., Menegazzo F. and Signoretto M. (2021). "A review on the efficient catalysts for algae transesterification to biodiesel." *Sustainability* **13**(18): 10479.

Gomaa A., Mohamed H., El Gwady A. and Al-Aseebee M. (2014). "Evaluation of tractor diesel engine performance using biodiesel from three different individual sources." *Misr Journal of Agricultural Engineering* **31**(2): 403–424.

Habibullah M., Masjuki H. H., Kalam M. A., Fattah I. R., Ashraful A. and Mobarak H. (2014). "Biodiesel production and performance evaluation of coconut, palm and their combined blend with diesel in a single-cylinder diesel engine." *Energy Conversion and Management* **87**: 250–257.

Hajjari M., Tabatabaei M., Aghbashlo M. and Ghanavati H. (2017). "A review on the prospects of sustainable biodiesel production: A global scenario with an emphasis on waste-oil biodiesel utilization." *Renewable and Sustainable Energy Reviews* **72**: 445–464.

Hezam I. M., Vedala N. R. D., Kumar B. R., Mishra A. R. and Cavallaro F. (2023). "Assessment of Biofuel industry sustainability factors based on the intuitionistic fuzzy symmetry point of criterion and rank-sum-based MAIRCA Method." *Sustainability* **15**(8): 6749.

Jia L., Cheng P., Yu Y., Chen S.-H., Wang C.-X., He L., Nie H.-T., Wang J.-C., Zhang J.-C. and Fan B.-G. (2023). "Regeneration mechanism of a novel high-performance biochar mercury adsorbent directionally modified by multimetal multilayer loading." *Journal of Environmental Management* **326**: 116790.

Kale P. T. (2017). "Combustion of biodiesel in CI engine." *Int. J. Appl. Res* **3**(3): 145–149.

Ketata A., Moussa O. and Driss Z. (2023). "Start of injection timing effect on performance and exhaust emissions of a combustion engine powered by a diesel-oleic acid methyl ester biodiesel blend." *International Journal of Ambient Energy* **44**(1): 515–526.

Lee S., Posarac D. and Ellis N. (2011). "Process simulation and economic analysis of biodiesel production processes using fresh and waste vegetable oil and supercritical methanol." *Chemical Engineering Research and Design* **89**(12): 2626–2642.

López A. F., Cadrazco M., Agudelo A. F., Corredor L. A., Vélez J. A. and Agudelo J. R. (2015). "Impact of n-butanol and hydrous ethanol fumigation on the performance and pollutant emissions of an automotive diesel engine." *Fuel* **153**: 483–491.

McCarthy P., Rasul M. and Moazzem S. (2011). "Comparison of the performance and emissions of different biodiesel blends against petroleum diesel." *International Journal of Low-Carbon Technologies* **6**(4): 255–260.

McCormick R., Alleman T. and Nelson R. (2023). *Statistical Treatise on Critical Biodiesel (B100) Quality Properties in the United States* from 2004-2022, SAE Technical Paper.

Musharavati F., Sajid K., Anwer I., Nizami A.-S., Javed M. H., Ahmad A. and Naqvi M. (2023). "Advancing biodiesel production system from mixed vegetable oil waste: a life cycle assessment of environmental and economic outcomes." *Sustainability* **15**(24): 16550.

Nathan S. S., Mallikarjuna J. and Ramesh A. (2010). "An experimental study of the biogas–diesel HCCI mode of engine

operation." *Energy Conversion and Management* **51**(7): 1347–1353.

Patel R. L. and Sankhavara C. (2017). "Biodiesel production from Karanja oil and its use in diesel engine: A review." *Renewable and Sustainable Energy Reviews* **71**: 464–474.

Rahman M. M., Kamil M. and Bakar R. A. (2011). "Engine performance and optimum injection timing for 4-cylinder direct injection hydrogen fueled engine." *Simulation Modelling Practice and Theory* **19**(2): 734–751.

Raju V. D., Veza I., Venu H., Soudagar M. E. M., Kalam M., Ahamad T., Appavu P., Nair J. N. and Rahman S. A. (2023). "Comprehensive analysis of compression ratio, exhaust gas recirculation, and pilot fuel injection in a diesel engine fuelled with tamarind biodiesel." *Sustainability* **15**(21): 15222.

Rattanaphra D., Tawkaew S., Chuichulcherm S., Kingkam W., Nuchdang S., Kitpakornsanti K. and Suwanmanee U. (2023). "Evaluation of life cycle assessment of jatropha biodiesel processed by esterification of thai domestic rare earth oxide catalysts." *Sustainability* **16**(1): 100.

Sanjid A., Kalam M., Masjuki H., Rahman S. A. and Abedin M. (2014). "Combustion, performance and emission characteristics of a DI diesel engine fueled with Brassica juncea methyl ester and its blends." *RSC Advances* **4**(70): 36973–36982.

Singh D., Sharma D., Soni S., Sharma S. and Kumari D. (2019). "Chemical compositions, properties, and standards for different generation biodiesels: A review." *Fuel* **253**: 60–71.

Sourmehi C. (2021). "EIA projects nearly 50% increase in world energy use by 2050, led by growth in renewables." *Today in Energy*: 1.

Srivastava E., Kesharvani S., Agrawal A. and Dwivedi G. (2023). "Binary blending of different types of biofuels with diesel, and study of engine performance, combustion and exhaust emission characteristics." *Materials Today: Proceedings* **78**: 378–389.

Vickram S., Manikandan S., Deena S., Mundike J., Subbaiya R., Karmegam N., Jones S., Yadav K. K., woong Chang S. and Ravindran B. (2023). "Advanced biofuel production, policy and technological implementation of nano-additives for sustainable environmental management–A critical review." *Bioresource Technology* **387**: 129660.

Vlysidis A., Binns M., Webb C. and Theodoropoulos C. (2011). "A techno-economic analysis of biodiesel biorefineries: assessment of integrated designs for the co-production of fuels and chemicals." *Energy* **36**(8): 4671–4683.

Zailani S., Iranmanesh M., Hyun S. S. and Ali M. H. (2019). "Barriers of biodiesel adoption by transportation companies: A case of Malaysian transportation industry." *Sustainability* **11**(3): 931.

Zayed A., SM Abd El-Kareem M. and Zaky N. (2016). "Gas chromatography-mass spectrometry studies of waste vegetable mixed and pure used oils and its biodiesel products." *Journal of Pharmaceutical and Applied Chemistry* **2**(1): 30–37.

Zhang Y., Yan Y., Yang R., Wang Q., Zhang B., Gan Q., Liu Z. and Fu J. (2022). "Study of in-cylinder heat transfer boundary conditions for diesel engines under variable altitudes based on the CHT model." *Frontiers in Energy Research* **10**: 828215.